

TERAHERTZ SPECTROSCOPY AND GLOBAL ANALYSIS OF THE ROTATIONAL SPECTRUM OF DOUBLY DEUTERATED AMIDOGEN RADICAL ND₂

MATTIA MELOSSO,¹ CLAUDIO DEGLI ESPOSTI,¹ AND LUCA DORE¹

¹*Dipartimento di Chimica "Giacomo Ciamician", Università di Bologna, via Selmi 2, 40126 Bologna, Italy*

(Received July 3, 2017; Revised September 13, 2017; Accepted October 6, 2017)

Submitted to ApJS

ABSTRACT

The deuteration mechanism of molecules in the interstellar medium (ISM) is still being debated. Observations of deuterium-bearing species in several astronomical sources represent a powerful tool to improve our understanding of the interstellar chemistry. The doubly deuterated form of the astrophysically interesting Amidogen radical could be a target of detection in space. In this work, the rotational spectrum of the ND₂ radical in its ground vibrational and electronic X^2B_1 states has been investigated between 588 and 1131 GHz using a frequency modulation millimeter/submillimeter-wave spectrometer. The ND₂ has been produced in a free-space glass absorption cell by discharging a mixture of ND₃ and Ar. Sixty-four new transition frequencies involving J values from 2 to 5 and K_a values from 0 to 4 have been measured. A global analysis including all the previous field-free pure rotational data has been performed, allowing for a more precise determination of a very large number of spectroscopic parameters. Accurate predictions of rotational transition frequencies of ND₂ are now available from a few GHz up to several THz.

Keywords: astrochemistry – ISM: molecules – methods: laboratory: molecular – molecular data – techniques: spectroscopic

arXiv:1712.00219v1 [astro-ph.GA] 1 Dec 2017

1. INTRODUCTION

Recent discoveries of multiply deuterated molecules in the interstellar medium (ISM) (Ceccarelli et al. 1998; Lis et al. 2002; Vastel et al. 2003; Parise et al. 2004) have confirmed the interest in deuterium-bearing species, since deuterium fractionation is a powerful tool to study the evolution of the Solar System (Millar 2002; Sandford 2002; Roueff et al. 2003). Both gas-phase models and active chemistry on grain-surface have been invoked to explain the formation of doubly or even triply deuterated species and their anomalous large amount (Roberts et al. 2000; Caselli 2002; Roberts et al. 2003). Further detections of multiply deuterated species are thus fundamental to constraint the chemical models and spectroscopic laboratory data are necessary to the goal.

The doubly deuterated Amidogen radical, ND₂, represents a possible target, since NH₂ is involved in the formation process of ammonia (Herbst et al. 1987) and all the deuterated isotopologues of ammonia have been detected in space (Turner et al. 1978; Roueff et al. 2000; Lis et al. 2002). The main isotopologue NH₂ was first observed in 1943 in a comet (Swing et al. 1943) by optical astronomy. More recently, it has also been detected via radio observation of the star-forming region Sagittarius B2 (van Dishoek et al. 1993) and of many other sources (Hily-Blant et al. 2010; Persson et al. 2010). Moreover, in 2015 the rare ¹⁵N-substituted isotopologue has been observed through cometary emissions (Rousselot et al. 2014; Shinnaka et al. 2014). However, no detection of deuterated Amidogen, even in its mono deuterated form NHD, has been reported to date.

Nevertheless, the existence of deuterated forms of Amidogen in ISM seems to be plausible as predicted by the gas-phase chemical models, in which the dissociative recombination of partially deuterated intermediates results in a higher probability for the ejection of a hydrogen atom than deuterium. Roueff et al. (2005) presented a steady state model of the gas phase chemistry aimed at understanding the deuterium fractionation of ammonia in various sources: these authors considered different physical conditions and could derive a general trend. At high density and high depletion, deuteration of N-containing species results very efficient at 10 K. Actually, the abundances of singly and multiply deuterated forms of H₃⁺ can reach exceptionally high values under conditions of extreme CO-depletion, and these high degrees of deuteration can propagate to the residual nitrogen-bearing species (Flower et al. 2006), that appear to be less depleted and subsist longer in the gas phase (see Bergin et al. (1997) and Belloche et al. (2004) for the cases of NH₃ and N₂H⁺, respectively).

The deuterium fractionation is sensitive to the temperature, but it remains large for temperatures between 5 and 20 K. Thus, the model predicts high fractional abundances of ammonia progenitors and their deuterated isotopologues, namely NH, ND, NH₂, NHD and ND₂, in dense cores. In general, the predicted abundance ratios of the deuterated ammonia isotopologues and their progenitors agree reasonably well with existing observations, and, noticeably, the fractional abundance of ND₂ is estimated to be from 2 to 9 times larger than the ND₃ abundance.

The ND₂ radical has been long studied with various spectroscopic techniques: electronic, Laser Magnetic Resonance (LMR), Microwave Optical Double Resonance (MODR), millimeter-wave (mmW) and Fourier-Transform Far InfraRed (FT-FIR) spectroscopy. Briefly, the rotational constants were first derived from the electronic spectrum (Dressler et al. 1959), while quartic centrifugal distortion and fine interaction parameters were obtained by means of LMR studies (Hills et al. 1979). Later on, Cook et al. (1983) determined the hyperfine coupling constants using MODR spectroscopy and Kanada et al. (1991) measured the pure rotational spectrum in the range 265 - 531 GHz using a submillimeter-wave spectrometer. Lastly, Morino et al. (1997) observed the far-infrared spectrum in the 102 - 265 cm⁻¹ region with a high-resolution FT spectrometer.

In the present work, newly observed rotational transitions from 588 GHz to 1.13 THz have been measured for ND₂ with microwave accuracy. A global analysis including also all previous field-free rotational data has been performed thus obtaining a considerably improved set of spectroscopic constants, from which more accurate predictions of transition frequencies of ND₂ can be produced in a wide range of its rotational spectrum.

2. EXPERIMENT

The rotational spectrum of ND₂ radical has been investigated in selected frequency regions between 588 GHz and 1.13 THz using a source-modulation millimeter/sub-millimeter wave spectrometer, as in Dore et al. (2017) and Bizzocchi et al. (2016). The main sources of radiation were several Gunn diodes (Radiometer Physics GmbH, J. E. Carlstrom Co) which emit in the 80-134 GHz frequency range. Higher frequencies were obtained by using passive doublers or triplers (RPG) in cascade. The sources were phase-locked to the suitable harmonic of a frequency synthesizer (Schomandl ND 1000) referenced to an external rubidium frequency standard. The frequency modulation of the radiation was obtained by sine-wave modulating at 6 kHz the reference signal of the wide-band Gunn

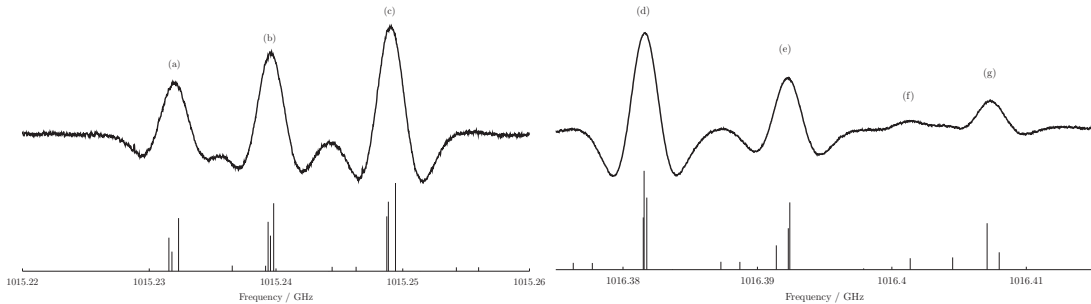


Figure 1. Observed and predicted frequencies for two fine components of the $N = 3_{13} \leftarrow 2_{02}$ transition at 1015-1016 GHz. Both scans were recorded with a RC constant of 3 ms and a total integration time of about 200 s. *Left panel:* $J = 3.5 \leftarrow 2.5$ (a) $(F_1 = 2.5 \leftarrow 1.5, F = 2.5 \leftarrow 1.5), (F_1 = 2.5 \leftarrow 1.5, F = 1.5 \leftarrow 0.5), (F_1 = 2.5 \leftarrow 1.5, F = 3.5 \leftarrow 2.5)$ (b) $(F_1 = 3.5 \leftarrow 2.5, F = 3.5 \leftarrow 2.5), (F_1 = 3.5 \leftarrow 2.5, F = 2.5 \leftarrow 1.5), (F_1 = 3.5 \leftarrow 2.5, F = 4.5 \leftarrow 3.5)$ (c) $(F_1 = 4.5 \leftarrow 3.5, F = 3.5 \leftarrow 2.5), (F_1 = 4.5 \leftarrow 3.5, F = 4.5 \leftarrow 3.5), (F_1 = 4.5 \leftarrow 3.5, F = 5.5 \leftarrow 4.5)$ *Right panel:* $J = 2.5 \leftarrow 1.5$ (d) $(F_1 = 3.5 \leftarrow 2.5, F = 2.5 \leftarrow 1.5), (F_1 = 3.5 \leftarrow 4.5, F = 2.5 \leftarrow 3.5), (F_1 = 3.5 \leftarrow 2.5, F = 3.5 \leftarrow 2.5)$ (e) $(F_1 = 2.5 \leftarrow 1.5, F = 1.5 \leftarrow 0.5), (F_1 = 2.5 \leftarrow 1.5, F = 2.5 \leftarrow 1.5), (F_1 = 2.5 \leftarrow 1.5, F = 3.5 \leftarrow 2.5)$ (f) $(F_1 = 1.5 \leftarrow 0.5, F = 1.5 \leftarrow 1.5)$ (g) $(F_1 = 1.5 \leftarrow 0.5, F = 2.5 \leftarrow 1.5), (F_1 = 1.5 \leftarrow 0.5, F = 1.5 \leftarrow 0.5)$

synchronizer. The absorption cell (3.25 m long, 5 cm in diameter) was equipped with two cylindrical hollow electrodes 25 cm in length at either end, and was wound with a plastic pipe for liquid nitrogen circulation. A liquid-helium-cooled InSb detector (QMC Instr. Ltd. type QFI/2) was used for detection. The radiation was phase-sensitively detected by a lock-in amplifier at twice the modulation frequency, so that the second derivative of the spectrum profile was displayed.

The ND₂ radical was produced with an electrical glow-discharge system. A mixture of ND₃ (5-7 mTorr) and Ar (20 mTorr) was used, as in Kanada et al. (1991). Typically, a discharge current of 70 mA and a voltage of about 1 kV were maintained between the electrodes while recording the spectrum. The absorption cell was cooled continuously just above the freezing point of ammonia with liquid nitrogen, in order to avoid an excessive overheating of the two electrodes. The estimated uncertainties of the measurements are 50 kHz in most cases, 100 kHz in a few cases. The accuracy depends on the signal to noise ratio of the observed spectrum and on line-blending due to unresolved hyperfine components.

3. RESULTS AND ANALYSIS

The ND₂ radical in its electronic ground state X^2B_1 is an asymmetric rotor of C_{2v} symmetry whose dipole moment (1.82 D) lies along the b axis (Brown et al. 1979). Because of the spin of the unpaired electron ($S = \frac{1}{2}$) and the spin of the ¹⁴N nucleus ($I_N = 1$), this radical shows a complex spectrum with fine and hyperfine structures (see Figure 1). In fact, each rotational level with quantum number $N \neq 0$ is split into two sublevels with $J = N + \frac{1}{2}$ and $J = N - \frac{1}{2}$ because of the coupling of the rotation with the electron spin. Each of these two sublevels is then split by the interaction with

the nuclear spin of ¹⁴N. A further splitting of the nitrogen hyperfine components is due to deuterium nuclear spin. Deuterium is a boson ($I_D = 1$), therefore the total wavefunction has to be symmetric upon exchange of the two identical nuclei, that is of A symmetry. Since the X^2B_1 electronic state is antisymmetric and the vibrational ground state is symmetric, then symmetric rotational levels ($K_{-1}K_1 = (ee)$ or (oo)) combine with antisymmetric deuterium spin functions, with $I_D = I_{D_1} + I_{D_2} = 1$, while antisymmetric rotational levels ($K_{-1}K_1 = (eo)$ or (oe)) combine with spin functions with $I_D = 0, 2$, which are symmetric upon exchange of the D nuclei. Thus the symmetric rotational levels are split in three further hyperfine sublevels and the antisymmetric ones in six sublevels. Therefore the coupling scheme used in the present work is the following:

$$\begin{aligned}\hat{J} &= \hat{N} + \hat{S} \\ \hat{F}_1 &= \hat{J} + \hat{I}_N \\ \hat{F} &= \hat{F}_1 + \hat{I}_D.\end{aligned}$$

The effective Hamiltonian for the ND₂ radical can be expressed as (Kanada et al. 1991; Morino et al. 1997):

$$\hat{H} = \hat{H}_{rot} + \hat{H}_{fs} + \hat{H}_{hfs}, \quad (1)$$

where \hat{H}_{rot} is the Watson A -reduced Hamiltonian in the I^r representation (Watson 1977), which includes the rotational energy and the centrifugal distortion terms. The fine-structure Hamiltonian \hat{H}_{fs} contains the electron spin-rotation terms with constants ϵ_{ii} and their centrifugal dependences. The \hat{H}_{hfs} operator is the hyperfine-structure Hamiltonian and can be separated into two components:

$$\hat{H}_{hfs} = \hat{H}_{hfs}(N) + \hat{H}_{hfs}(D). \quad (2)$$

In the present analysis, the effect of isotropic (a_F) and anisotropic (T_{ii}) electronic spin-nuclear spin coupling constants were considered for both nuclei, while electric quadrupole (eQq) and spin-rotation (C_{ii}) coupling constants could be determined only for the ^{14}N -nitrogen nucleus.

The initial predictions were made using the Pickett's program SPCAT (Pickett 1991) with the constants derived by Kanada et al. (1991). The production of ND_2 was optimized by observing the $J = 0 \leftarrow 0$ component of the $N = 1_{10} \leftarrow 1_{01}$ transition. Then, the fine components of new eight rotational transitions were recorded and their hyperfine structure could be easily assigned thanks to the already known hyperfine-interaction parameters. Sixty-four distinct frequencies were measured and analyzed in a weighted least-squares procedure, in which previous data (millimeter/sub-millimeter, MODR and FIR studies) were included. In this procedure, performed with the Pickett's program SPFIT (Pickett 1991), the mmW and sub-mmW lines previously measured by Kanada et al. (1991) were given uncertainties of 50 kHz, whereas the FIR data from Morino et al. (1997) were given uncertainties of 0.0007 cm^{-1} , as in the analysis of NH_2 (Müller et al. 1999). For the MODR data (Cook et al. 1983) the same uncertainties given in the original work were assumed (typically 0.5 MHz). Surprisingly, the older sets of frequency data were never analyzed simultaneously, so that different sets of spectroscopic constants, not fully consistent, have been reported in the literature for ND_2 . The present global analysis allows to obtain spectroscopy constants which are compatible with the entire body of rotational data available for this radical. Moreover, we were able to complete and/or correct previous assignments. As far as MODR data are concerned, about 20% of the observed transitions were not considered in the fit of Cook et al. (1983) because of the failure to unambiguously assign their hyperfine components. Our more extensive data analysis allowed us to overcome this difficulty, so that a large number of previously unused MODR frequencies could be included in our fit. Furthermore, during the merging process some FIR transitions appeared to be misassigned, so they have been reassigned correctly in this study. In particular, a few transitions with $N \geq 10$ had been wrongly assigned as $\Delta K_a = \pm 3$ instead of $\Delta K_a = \pm 1$. In the final fit, unresolved lines were treated using the intensity-weighted average of the individual components involved. A total number of 41 spectroscopic constants were included in the least squares analysis, giving a satisfactory dimensionless standard deviation of 0.87. Table 1 shows the list of spectroscopic parameters determined in the present work, where they

are compared to those obtained previously. In general, all derived parameters are determined with higher precision than in the previous works: for instance, the standard errors of the rotational constants are one order of magnitude lower and the hyperfine constants are three times more precise. This is mainly due to the simultaneous analysis of MW spectroscopy measurements (high frequency precision and resolving power) with FT-FIR data (large range of N and K_a quantum numbers). The newly determined values of the spectroscopic constants agree well with those previously reported by Kanada et al. (1991) and Morino et al. (1997), the only exceptions being ϕ_K and l_K . This discrepancy should be ascribed to the reassignment process of some FIR transitions (see above).

It is well known that the lightness and non-rigidity of triatomic hydrides of C_{2v} symmetry (e.g. CH_2 , H_2O , NH_2) cause abnormal centrifugal distortion effects (Brünken et al. 2005; Yu et al. 2012; Martin-Drumel et al. 2014), so that describing the rotational energy levels using a Watson-type Hamiltonian presents some difficulties due to the slow convergence of the standard power series expansion of the rotational angular momentum operators. As a matter of fact, a huge number of centrifugal distortion terms (mainly K_a dependent) has to be included in the Hamiltonian model in order to reproduce highly accurate rotational data within their experimental uncertainty. This difficulties are less pronounced for the heavier doubly deuterated isotopologues, for which the centrifugal distortion effects are smaller. As far as the Amidogen radical is concerned, on the average the quartic centrifugal distortion constants determined for ND_2 are ca. three times smaller than those of NH_2 , and the sextic ones ca. seven times smaller (Martin-Drumel et al. 2014). No problem of convergence has been experienced in the present analysis using the standard semi-rigid Hamiltonian, so that the experimental transition frequencies could be satisfactorily reproduced ($\sigma = 0.87$) using, as fit parameters, 16 centrifugal distortion constants less than in the case of NH_2 (Martin-Drumel et al. 2014). For this reason no other form of the rotational Hamiltonian was considered for the analysis.

Table 2 provides an example of the machine-readable table included as Electronic Supplementary Information. Files used with the SPFIT/SPCAT program suite are also included as supplementary materials. These files can be used to predict the rotational spectrum at a given temperature and in selected frequency regions. It should be noted that the prediction of transition frequencies corresponding to quantum numbers higher than those involved in the present analysis (i.e. $N > 13$

Table 1. Spectroscopic parameters derived for ND₂

Constants	Present work	Previous MW ^a	Previous FIR ^b
A	/MHz 399989.5534(87) ^c	399985.879(81)	399993.92(189)
B	/MHz 194498.1916(150)	194488.65(16)	194498.10(102)
C	/MHz 128610.4447(145)	128613.987(57)	128610.00(126)
Centrifugal distortion			
Δ_N	/MHz 7.86074(33)	7.323(10)	7.8392(108)
Δ_{NK}	/MHz -33.48376(259)	-33.812(25)	-33.388(42)
Δ_K	/MHz 198.7064(57)	196.771(33)	198.783(84)
δ_N	/MHz 3.080801(201)	3.03 ^d	3.0858(36)
δ_K	/MHz 8.5567(82)	6.300(39)	8.2788(294)
Φ_N	/kHz 1.4776(80)		1.376(35)
Φ_{NNK}	/kHz -6.277(306)		-5.606(35)
Φ_{KKK}	/kHz -43.70(98)		-43.45(96)
Φ_K	/kHz 320.34(90)		321.0(23)
ϕ_N	/kHz 0.7224(33)		0.7402(140)
ϕ_{NK}	/kHz -0.834(99)		-1.01(21)
ϕ_K	/kHz 65.90(133)		33.37(65)
L_{KKKN}	/kHz 0.08336(141)		0.0707(38)
L_K	/kHz -0.7022(85)		-0.694(26)
l_K	/kHz -0.1230(33)		-0.0311(16)
M_K	/Hz 1.069(38)		1.08(10)
Fine interaction			
ϵ_{aa}	/MHz -5128.1262(215)	-5127.81(11)	-5127.71(41)
ϵ_{bb}	/MHz -668.6973(180)	-668.507(78)	-668.759(160)
ϵ_{cc}	/MHz 3.4616(166)	3.413(63)	3.23(12)
Δ_N^S	/MHz 0.07613(57)	0.0469(66)	0.0779(29)
Δ_{KN+NK}^S	/MHz -0.9498(57)	-0.967(81)	-0.875(29)
Δ_{NK}^S	/MHz 1.045(201)		
Δ_K^S	/MHz 9.8548(76)	9.587(66)	9.476(99)
δ_N^S	/MHz 0.03843(36)		0.0353(16)
δ_K^S	/MHz 0.1005(59)	0.0356(45)	0.150(36)
Φ_{NKK}^S	/kHz 3.76(51)		
Φ_K^S	/kHz -23.10(81)		-15.36(72)
Hyperfine interaction			
$a_F(N)$	/MHz 28.0577(122)	28.055(33)	
$T_{aa}(N)$	/MHz -43.1451(183)	-43.136(48)	
$T_{bb}(N)$	/MHz -44.2715(213)	-44.277(63)	
$C_{aa}(N)$	/MHz 0.2660(75)	0.269(27)	
$C_{bb}(N)$	/MHz 0.0458(55)	0.045(21)	
$C_{cc}(N)$	/MHz 0.0145(64)	0.019(22)	
$a_F(D)$	/MHz -10.2446(103)	-10.241(28)	
$T_{aa}(D)$	/MHz 2.8536(168)	2.874(45)	
$T_{bb}(D)$	/MHz -2.0916(247)	-2.108(69)	
$X_{aa}(N)$	/MHz 0.2191(297)	0.213(84)	
$X_{bb}(N)$	/MHz -3.744(34)	-3.75(11)	
Number of FIR lines			181
Standard deviation of the FIR data /cm ⁻¹			6.9 × 10 ⁻⁴
Number of MODR lines			198
Standard deviation of the MODR data /MHz			0.376
Number of MW lines			182
Standard deviation of the MW data /kHz			51.0
Fit standard deviation			0.87
N'_{max}, K'_{max}			13, 10

^a Kanada et al. (1991)

^b Morino et al. (1997). The values, originally reported in cm⁻¹, are converted to MHz.

^c Values in parenthesis denote one standard deviation and apply to the last digits.

^d Fixed

and $K_a > 10$) could be affected by systematic errors due to the truncation of the slowly convergent power series expansion of the standard semi-rigid Hamiltonian. It is not easy to make an *a priori* evaluation of the magnitude of these model-dependent errors, however an estimate of the convergence radius of a power series can provide useful information (Brünken et al. 2005). For instance, considering the series of the purely K_a dependent centrifugal distortion terms, $\sum_n c_n (K_a^2)^n$, its convergence radius is the inverse square-root of the absolute value of $\lim_{n \rightarrow \infty} c_n/c_{n-1}$, which can be estimated from the intercept of the plot of c_n/c_{n-1} versus $1/n$. For the present centrifugal analysis, a convergence radius of $K_a = 17$ results: at this value of K_a , $|c_{n-1}| (K_a^2)^{n-1} \sim |c_n| (K_a^2)^n$ holds, therefore the missing higher order term gives a substantial contribution to the energy of the level. In conclusion, the semi-rigid Hamiltonian with the present set of constants is fully accurate to predict the ND₂ spectrum for $K_a \leq 10$, it is still appropriate, with less accuracy, for $10 < K_a \leq 17$, but for $K_a > 17$ no reliable predictions of the spectrum can be obtained.

4. CONCLUSION

The rotational spectrum of the doubly deuterated variant of Amidogen radical ND₂ in its ground electronic state X^2B_1 has been investigated in the frequency region 588 - 1131 GHz. New measurements have been analyzed in a global fit including previous mmW, sub-mmW, MODR and FIR data. Some misassignments or incomplete assignments of previous data sets have been corrected, so that it has been possible to obtain a set of very accurate spectroscopy constants which are compatible with the entire body of rotational data presently available for this radical. Accurate predictions are now available up to 8 THz for those transitions with $N \leq 13$ and $K_a \leq 10$. This work provides a facility set of data for the radio-observation of fully deuterated Amidogen radical.

5. ACKNOWLEDGMENTS

This study was supported by Bologna University (RFO funds) and by MIUR (Project PRIN 2015: STARS in the CAOS, Grant Number 2015F59J3R).

REFERENCES

- Belloche, A., & André, P. 2004, *A&A*, 419, L35-L38
- Bergin, E. A., & Langer, W. D. 1997, *ApJ*, 486, 316-328
- Bizzocchi, L., Dore, L., Degli Esposti, C., & Tamassia, F. 2016, *ApJL*, 820, L26
- Brown, J. M., Chalkley, S. W., & Wayne, F. D. 1979, *Mol. Phys.*, 38, 1521-1537
- Brünken, S., Müller, H. S. P., Lewen, F., & Giesen, T., 2005, *J. Chem. Phys.*, 123, 164315 (10pp)
- Caselli, P., Stantcheva, T., Shalabeia, O., Shematovich, V. I., & Herbst, E. 2002, *Planetary and Space Science*, 50, 1257-1266
- Ceccarelli, C., Castets, A., Loinard, L., Caux, E. & Tielens, A. G. G. M. 1998, *A&A*, 338, L43-L46
- Ceccarelli, C., Caselli, P., Bockele-Morvan, D., et al. 2014, *Protostars and Planets VI*, 859
- Cook, J. M. & Hills, G. W. 1983, *J. Chem. Phys.*, 78, 2144
- Dore, L., Bizzocchi, L., Wirström, E. S., Degli Esposti, C., Tamassia, F. & Charnley, S. B. 2017, *A&A*, 604, A26
- Dressler, K. & Ramsay, D. A. 1959, *Philos. Trans. R. Soc. London A*, 251, 553
- Flower, D. R., Pineau des Forêts, G., & Walmsley, C. M. 2006, *A&A*, 449, 621-629
- Herbst, E., DeFrees, D. J., & McLean, A. D. 1987, *ApJ*, 321, 898-906
- Hills, G. W. & McKellar, A. R. W. 1979, *J. Chem. Phys.*, 71, 3330
- Hily-Blant, P., et al., 2010, *A&A*, 521, L52
- Kanada, M., Yamamoto, S., & Saito, S. 1991, *J. Chem. Phys.*, 94, 3423
- Lis, D. C., Roueff, E., Gerin, M., Phillips, T. G., Coudert, L. H., Van Der Tak, F. F. S., & Schilke, P. 2002, *ApJ*, 75, L55-L58
- Martin-Drumel, M. A., Pirali, O., and Vervloet, M. 2014, *J. Phys. Chem. A*, 118, 1331-1338
- Millar, T. J. 2002, *Planetary and Space Science*, 50, 1189-1195
- Morino, I. & Kawaguchi, K. 1997, *J. Mol. Spectrosc.*, 182, 428-438
- Müller, H. S. P., Klein, H., Belov, S. P., Winniewisser, G., Morino, I., Yamada, K. M. T., & Saito, S. 1999, *J. Mol. Spectrosc.*, 195, 177-184
- Parise, B., Castets, A., Caux, E., Ceccarelli, C., Mukhopadhyay, I., & Tielens, A. G. G. M. 2004, *A&A*, 416, 159-163
- Persson, C. M., et al., 2010, *A&A*, 521, L45
- Pickett, H. M. 1991, *J. Mol. Spectrosc.*, 148, 371-377
- Roberts, H., & Millar, T. J. 2000, *A&A*, 364, 780-784
- Roberts, H., Herbst, E., & Millar, T. J. 2003, *ApJ*, 591, L41-L44

Table 2. Observed frequencies and residual from the final fit for ND₂ Amidogen radical

N'	K'_a	K'_c	J'	F'_1	I'_D	F'	N	K_a	K_c	J	F_1	I_D	F	Obs. Frequency (MHz)	Uncert. (MHz)	Obs.-Calc. (MHz)	Relative weight ^a	Reference
3	1	3	4	3	1	3	2	0	2	3	2	1	2	1015231.991	0.050	0.016	0.3157	This work
3	1	3	4	3	1	2	2	0	2	3	2	1	1	1015231.991	0.050	0.016	0.1845	This work
3	1	3	4	3	1	4	2	0	2	3	2	1	3	1015231.991	0.050	0.016	0.4998	This work
3	1	3	4	4	1	4	2	0	2	3	3	1	3	1015239.596	0.050	-0.023	0.3230	This work
3	1	3	4	4	1	3	2	0	2	3	3	1	2	1015239.596	0.050	-0.023	0.2326	This work
3	1	3	4	4	1	5	2	0	2	3	3	1	4	1015239.596	0.050	-0.023	0.4445	This work
3	1	3	4	5	1	4	2	0	2	3	4	1	3	1015249.043	0.050	-0.023	0.2580	This work
3	1	3	4	5	1	5	2	0	2	3	4	1	4	1015249.043	0.050	-0.023	0.3270	This work
3	1	3	4	5	1	6	2	0	2	3	4	1	5	1015249.043	0.050	-0.023	0.4150	This work

NOTE—Table 2 is published in its entire form in the electronic edition of the ApJS. A portion is shown here for guidance regarding its form and content.

^aFor blended transitions

Roueff, E., Tin, S., Coudert, L. H., Pineau des Forets, G., Falgarone, E., & Gerin, M. 2000, *A&A*, 354, L63-L66
 Roueff, E., & Gerin, M. 2003, *Space Science Reviews*, 106, 61-72
 Roueff, E., Lis, D. C., van der Tak, F. F. S., Gerin, M., & Goldsmith, P. F. 2005, *A&A*, 438, 585-598
 Rousselot, P., Pirali, O., Jehin, E., et al., 2014, *ApJ*, 780, L17
 Sandford, S. A. 2002, *Planetary and Space Science*, 50, 1145-1154
 Shinnaka, Y., Kawakita, H., Kobayashi, H., Nagashima, M., & Boice, D. C. 2014, *ApJ*, 782, L16

Swing, P., McKellar, A., & Minkowski, R. 1943, *Astrophys. J.*, 95, 142
 Turner, B. E., Zuckerman, B., Morris, M., & Palmer, P. 1978, *ApJ*, 219, L43-L47
 van Dishoek, E. F., Jansen, D. J., Schilke, P., & Philips, T. G. 1993, *ApJ*, 416, L83-L86
 Vastel, C., Phillips, T. G., Ceccarelli, C., & Pearson, J. 2003, *ApJ*, 593, L97-L100
 Watson, J. K. G. 1977, *Vibrational Spectra and Structure*, vol. 6, pp.1-89 (Amsterdam: Elsevier)
 Yu, S., Pearson, J. C., Drouin, B. J., Martin-Drumel, M. A., Pirali, O., Vervloet, M., Coudert, L. H., Müller, H. S. P., & Brünken, S. 2012, *J. Mol. Spectrosc.*, 279, 16-25